BBA - Molecular Basis of Disease 1865 (2019) 165551

Contents lists available at ScienceDirect

BBA - Molecular Basis of Disease

journal homepage: www.elsevier.com/locate/bbadis

Chronic inhibition of chemokine receptor CXCR2 attenuates cardiac remodeling and dysfunction in spontaneously hypertensive rats

Yun-Long Zhang[a,1], Chi Geng[b,1], Jie Yang[b], Jiao Fang[b], Xiao Yan[b], Pang-Bo Li[a], Lei-Xin Zou[b], Chen Chen[b], Shu-Bin Guo[a], Hui-Hua Li[a,*], Ying Liu[b,*]

[a] Department of Emergency Medicine, Beijing Key Laboratory of Cardiopulmonary Cerebral Resuscitation, Beijing Chaoyang Hospital, Capital Medical University, Beijing 100020, China
[b] Department of Cardiology, Institute of Cardiovascular Diseases, First Affiliated Hospital of Dalian Medical University, Dalian 116011, China

ARTICLE INFO

Keywords:
Chemokine receptor CXCR2
Spontaneously hypertensive rats
Cardiac remodeling
Inflammation
Oxidative stress
Macrophage infiltration

ABSTRACT

System hypertension is a major risk factor for cardiac hypertrophy and heart failure. Our recent findings reveal that the ablation or inhibition of C-X-C chemokine receptor (CXCR) 2 blocks this process in mice; however, it is not clear whether the pharmacological inhibition of CXCR2 attenuates hypertension and subsequent cardiac remodeling in spontaneously hypertensive rats (SHRs). In the present study, we showed that chemokines (CXCL1 and CXCL2) and CXCR2 were significantly upregulated in SHR hearts compared with Wistar–Kyoto rat (WKY) hearts. Moreover, the administration of CXCR2-specific inhibitor *N*-(2-hydroxy-4-nitrophenyl)-*N′*-(2-bromophenyl)-urea (SB225002) in SHRs (at 2 months of age) for an additional 4 months significantly suppressed the elevation of blood pressure, cardiac myocyte hypertrophy, fibrosis, inflammation, and superoxide production and improved heart dysfunction in SHRs compared with vehicle-treated SHRs. SB225002 treatment also reduced established hypertension, cardiac remodeling and contractile dysfunction. Moreover, CXCR2-mediated increases in the recruitment of Mac-2-positive macrophages, proinflammatory cytokines, vascular permeability and ROS production in SHR hearts were markedly attenuated by SB225002. Accordingly, the inhibition of CXCR2 by SB225002 deactivates multiple signaling pathways (AKT/mTOR, ERK1/2, STAT3, calcineurin A, TGF-β/Smad2/3, NF-κB-p65, and NOX). Our results provide new evidence that the chronic blocking of CXCR2 activation attenuates progression of cardiac hypertrophic remodeling and dysfunction in SHRs. These findings may be of value in understanding the benefits of CXCR2 inhibition for hypertensive cardiac hypertrophy and provide further support for the clinical application of CXCR2 inhibitors for the prevention and treatment of heart failure.

1. Introduction

Hypertension is a major cause of both cardiac hypertrophy and heart failure (HF), which are associated with increased interstitial fibrosis, myocyte death, and cardiac contractile dysfunction. Accordingly, many antihypertensive drugs, including angiotensin II receptor inhibitors (ARBs), angiotensin II-converting enzyme inhibitors (ACEIs), and β-adrenaline receptor blockers have the ability to delay or reduce the development of cardiac hypertrophy [1]. The pathogenesis of cardiac remodeling can be influenced by multiple factors. Among these factors, inflammatory response and oxidative stress play critical roles in this process [2,3]. Hypertensive stimuli, such as Ang II or high salt, can induce inflammatory cell infiltration and cytokine production, such as tumor necrosis factor (TNF)-α, interleukin (IL)-1, and IL-6-related cytokines, which alter a variety of cellular signaling pathways, including serine/threonine kinase B (AKT)/mammalian target of rapamycin (mTOR), extracellular regulated protein kinases (ERK)1/2, signal transducers and activators of transcription (STAT)3, calcineurin (CaN) A, and transforming growth factor-β (TGF-β)/mothers against decapentaplegic homolog (Smad)2/3, thereby contributing to progressive cardiac remodeling and dysfunction [4–7].

Chemokines represent a large family of chemotactic proteins than control the recruitment of immune cells into injured tissues. In humans, chemokines are classified into four subfamilies, CXC, CC, XC, and CX3C based on the arrangement of cysteine residues at the N terminus [8]. In general, CC-chemokines are potent chemoattractants for monocytes, whereas CXC-chemokines are chemoattractants of neutrophils or lymphocytes [8]. Several studies have suggested that CXCL1 and its

* Corresponding authors.
E-mail addresses: hhli1935@aliyun.com (H.-H. Li), yingliu.med@gmail.com (Y. Liu).
[1] These authors contributed equally to this study.

https://doi.org/10.1016/j.bbadis.2019.165551
Received 1 February 2019; Received in revised form 23 August 2019; Accepted 4 September 2019
Available online 05 September 2019
0925-4439/

receptor C-X-C chemokine receptor (CXCR)2 have important roles in the pathogenesis of cardiovascular diseases, such as atherosclerosis, myocarditis, and ischemia/reperfusion injury [9–12]. We have recently demonstrated that CXCL1 or CXCR2 levels are elevated in Angiotensin (Ang) II-infused mice and patients with HF. The ablation or inhibition of CXCR2 attenuates monocyte recruitment, hypertension, and cardiac remodeling in mice [13,14]. However, whether the pharmacological inhibition of CXCR2 can effectively prevent or cure hypertension and cardiac remodeling remains to be validated in other animal models.

In this study, we explored the effects of the CXCR2 inhibitor SB225002 on macrophage recruitment and cardiac remodeling in a well-established model of hypertension and left ventricular (LV) hypertrophy in spontaneously hypertensive rats (SHRs). Our results showed, for the first time, that the expression levels of CXCL1 and CXCR2 are significantly higher in heart tissues of SHRs than in Wistar–Kyoto rat (WKY) controls. The administration of SB225002 to SHRs markedly prevented and reversed blood pressure elevation, cardiac remodeling, and dysfunction. These effects were associated with the inhibition of macrophage infiltration and multiple signaling pathways. Therefore, these results may be of value in understanding the benefits of CXCR2 inhibition for hypertensive cardiac hypertrophy and provide further support for the clinical applications of CXCR2 inhibitors for the prevention and treatment of HF.

2. Materials and methods

2.1. Animals and treatment

SHRs and aged-matched WKYs at 2 months of age (weight, 240–280 g) were obtained from Vital River Co., Ltd. (Beijing, China). Rats were kept in a conditioned room at 24 °C–25 °C under a 12-h light/dark cycle. Rat were given free access to standard rat chow and tap water ad libitum. For 6-month experiments, both WKYs and SHRs at 2 months of age were first evaluated by echocardiography (baseline), and then randomly divided into 4 groups, WKYs + vehicle, SHRs + vehicle, WKYs + SB225002 and SHRs + SB225002 (n = 8 per group). A selective CXCR2 inhibitor SB225002 (Selleck, Houston, TX, USA) or vehicle was administered intraperitoneally (1 $mg{\cdot}kg^{-1}\,day^{-1}$) at 2 months of age and continued for an additional 4 months. At end of 6 months, echocardiography was then performed and results were shown in Table S4. All animals were then sacrificed for histological examinations. For 11-month experiments, which tested the effect of CXCR2 inhibition on established cardiac remodeling, both WKYs and SHRs at 6 months of age were first evaluated by echocardiography (baseline), and then randomly divided into 4 groups, WKYs + vehicle, SHRs + vehicle, WKYs + SB225002 and SHRs + SB225002 (n = 8 per group). SB225002 or vehicle was administered intraperitoneally (1 $mg{\cdot}kg^{-1}\,day^{-1}$) at 6 months of age and continued for additional 5 months. At end of 11 months, echocardiography was then performed and results were shown in Table S5. All animals were then sacrificed for histological examinations. All animal experimental protocols conformed to the US National Institutes of Health Guide for the Care and Use of Laboratory Animals and were approved by the review board of the Animal Care and Use Committee of Dalian Medical University (AEE1-2016-045).

2.2. Blood pressure measurement

The blood pressure of peripheral arteries in rats was detected at 2 months and every week at the tail arteries by the noninvasive tail-cuff system (BP-2010A; Softron, Tokyo, Japan) using a preheated 37 °C plate to dilate the tail artery, as described previously [14,15].

2.3. Echocardiographic assessment

Cardiac structure and function were evaluated by transthoracic echocardiography using a Vevo 2100 High-Resolution Imaging System (Visual Sonics Inc., Toronto, Canada) by an experienced technician who was blinded to the animal groups, as previous reported [13,16]. Rats were weighed and anesthetized with 1.5% isoflurane. M-mode cardiac images of the left ventricle from the short-axis view were used to analyze chamber size, ventricular wall thickness, left ventricular posterior wall end-diastolic and end-systolic thicknesses (LVPW;d and LVPW;s), interventricular septal end-diastolic (IVS;d), heart rate (HR), ejection fraction (EF), and fractional shortening (FS) [13,16]. Pulse-wave Doppler images of mitral inflow from the apical 4-chamber view was used to detect the transmitral E/A ratio, an index of LV diastolic parameters [17].

2.4. Histological analyses

Rats hearts in each group were excised, and the heart weight (HW) to the body weight (BW) ratios were obtained. Left ventricles from each group were fixed in 10% formalin and embedded in liquid paraffin. Other myocardial tissue samples were fixed in paraformaldehyde, embedded in paraffin, and cut (5 μm), as described previously [13]. The sections were stained with hematoxylin and eosin, Masson's trichrome, and Rhodamine-labeled Wheat Germ Agglutinin (Vector Laboratories, Burlingame, CA, USA). Immunohistochemical staining was performed on the sections with alpha-Smooth Muscle Actin (α-SMA, Abcam, Cambridge, MA, USA) and Mac-2-antibodies (Santa Cruz, Dallas, Texas, USA). Immunofluorescence staining was performed on the sections with CXCR2 (Abcam, Cambridge, MA, USA), CD68 (Abcam, Cambridge, MA, USA), CD31(Santa Cruz, Dallas, Texas, USA), ZO-1 (Thermo, Carlsbad, CA, USA) and DAPI (Thermo, Carlsbad, CA, USA). Additionally, frozen sections of hearts (5 μm thick) were stained with dihydroethidine (Sigma-Aldrich, St. Louis., MO, USA) for 30 min at 37 °C [18]. The areas of cardiac myocyte surface, fibrosis, and $\alpha\text{-SMA}^+$, $CXCR2^+$, and $Mac\text{-}2^+$ cells and ZO-1-postive areas were analyzed using a fluorescence microscope (Nikon, Tokyo, Japan) and Image J, as described previously [13].

2.5. Quantitative real-time PCR analysis

Total tissue RNA was purified from hearts using TRIzol (Invitrogen, Carlsbad, CA, USA), and cDNA was synthesized using the GoScript TM reverse transcription system (Promega, Southampton, UK). Quantitative real-time PCR (qPCR) was performed using SYBR Green Master Mix (Takara, Kusatsu, Japan) on the Applied Biosystems 7500 Fast System (ABI, Carlsbad, CA, USA) as described previously [13,19]. *GAPDH* was used as an internal control. The primers were obtained from Sangon Biotech (Shanghai, China). Relative mRNA levels were calculated using the $2^{\Delta\Delta Ct}$ method as described previously [13,19]. The primer sequences are shown in Supplemental Table 1.

2.6. Immunoblotting analysis

Total protein was extracted from heart tissues using lysis buffer containing protease/phosphatase inhibitors (Thermo Fisher Scientific, Carlsbad, CA, USA). Protein concentrations were then assessed using the Abbkine Protein Quantification Kit (Thermo Fisher Scientific, Carlsbad, CA, USA). Equal amounts of proteins (40–50 μg) were separated by sodium dodecyl sulfate-polyacrylamide gel electrophoresis (SDS-PAGE) and transferred onto a polyvinylidene fluoride (PVDF) membrane (Millipore, Billerica, MA, USA). Immunoblotting analysis was performed as described previously [13,20]. All protein levels were normalized to GAPDH. Images were captured and quantified by FluorChem M (ProteinSimple, San Jose, CA, USA). The primary antibodies were as follows: CXCR2 (ab14935), nicotinamide adenine dinucleotide phosphate oxidase (NOX)1 (ab131088), NOX2 (ab129068), NOX4 (ab133303), and α-SMA (ab7817) from Abcam; Phospho-nuclear factor kappa-B (NF-κB)-p65 (3033S), NF-κB-p65 (4764S), Phospho-AKT

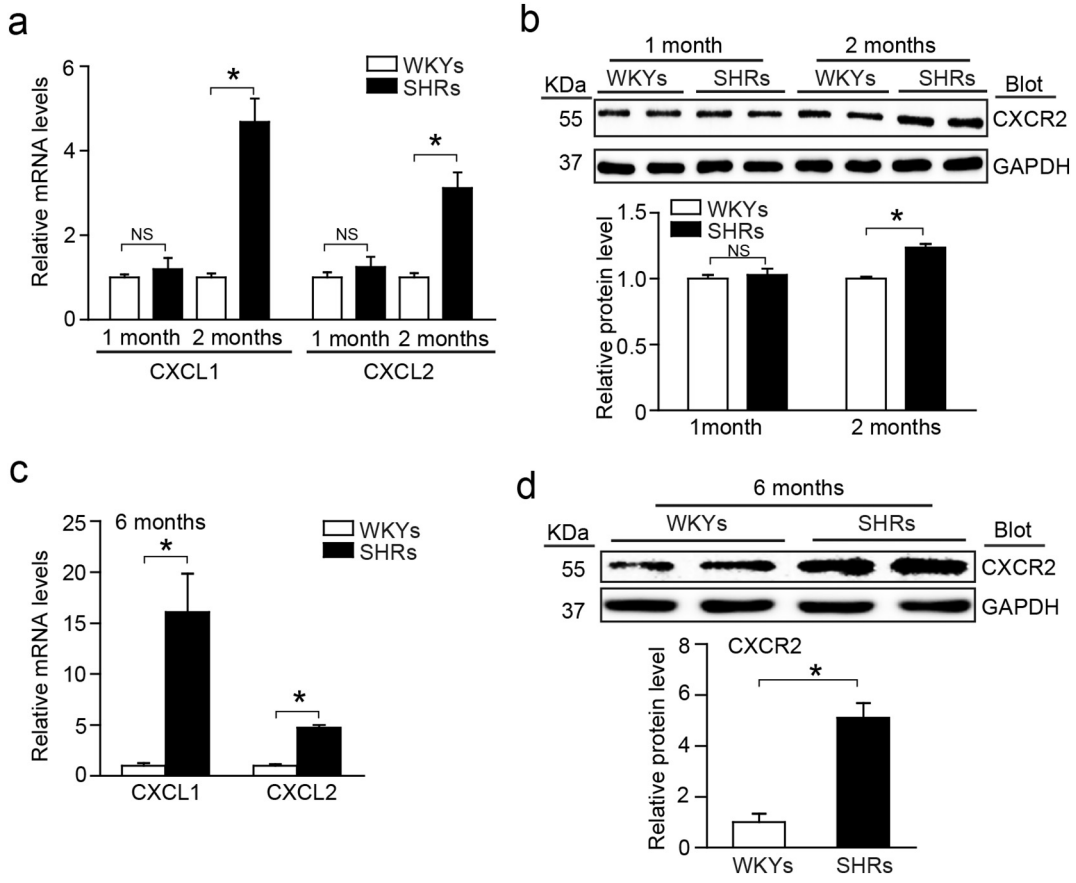

Fig. 1. Upregulation of CXCL1 and CXCR2 expression in the heart of SHRs. (a) qPCR analysis of CXCL1 and CXCL2 mRNA level in the hearts of Wistar-Kyoto (WKY) rats and spontaneously hypertensive rats (SHRs) at 2 months of age (n = 6). (b) Immunoblotting analysis of CXCR2 protein level in the hearts of WKYs and SHRs (top) and quantification of protein bands (bottom, n = 6). (c) qPCR analysis of CXCL1 and CXCL2 mRNA level in the hearts of Wistar-Kyoto (WKY) rats and spontaneously hypertensive rats (SHRs) at 6 months of age (n = 6). (d) Immunoblotting analysis of CXCR2 protein level in the hearts of WKYs and SHRs at 6 months of age (top) and quantification of protein bands (bottom, n = 6). Data are presented as means ± SEM, and n represents number of animals, $^{*}P < 0.05$ versus WKY; $^{ns}P > 0.05$ versus SHR.

(9271S), AKT (9272S), Phospho-STAT3 (9131S), STAT3 (8768S), Phospho-ERK1/2 (4370S), ERK1/2 (4695S), Pan-calcineurin A (2614S), TGF-β1 (3711S), Phospho-Smad2/3 (8828S), Smad2/3 (8685S), and GAPDH (2118S) from Cell Signaling Technology (Danvers, MA, USA). ZO-1 (61–7300) was from Thermo Fisher Scientific (Carlsbad, CA, USA).

2.7. Statistical analysis

Statistical calculations were performed using SPSS version 11.0. All data are presented as means ± SEM unless otherwise indicated in the figure legends. Sample sizes and experimental repeats are shown in figures and figure legends or in the Materials and methods section above. When data satisfied the assumptions of normality and equal variances, the student *t*-test was used to determine the significant difference between two groups. ANOVA was used for comparison between more than two groups. Differences in means were considered statistically significant at $P < 0.05$.

3. Results

3.1. CXCL1 and CXCR2 expression is increased in the heart of SHRs

We evaluated CXCL1 and CXCR2 expression levels in the hearts of SHRs by qPCR and immunoblotting at different time points (1, 2, and 6 months of age). Blood pressure increased as time progressed (up to 6 months) (Fig. 1a). Consistent with our previous results using Ang II-infused mice [13], the mRNA expression levels of CXCL1 and CXCL2 as well as the protein levels of CXCR2 were significantly higher in SHR hearts in the WKY hearts at 2 and 6 months (Fig. 1a–d). To determine whether blood pressure or the activation of angiotensin type 1 receptor (AT1R) increased CXCR2 expression and macrophage accumulation in the hearts, SHRs were treated with the AT1R antagonist candesartan for 6 months. We found that the blood pressure elevation, Mac-2^{+} macrophage counts, and mRNA levels of IL-1β, IL-6, and TNF-α in SHR hearts were significantly higher than those in WKY controls, but these increases were markedly reduced by candesartan (Supplemental Fig. 1a–d). Moreover, the protein levels of CXCR2 were also reduced in candesartan-treated SHR hearts (Supplemental Fig. 1e). However, the treatment of SHRs with the CXCR2 inhibitor SB225002 did not affect the AT1R protein level in the hearts (Supplemental Fig. 1f), suggesting that CXCR2 is a downstream mediator of AT1R. These results indicate that CXCR2-mediated macrophage infiltration is dependent on blood pressure in SHRs.

3.2. Administration of CXCR2 inhibitor attenuates hypertension and cardiac dysfunction in SHRs

Previous results have indicated that SHRs have a mild blood pressure at 2 months of age and display a compensatory increase in concentric left ventricular hypertrophy [21]. To determine the effect of CXCR2 inhibition in hypertensive hearts, we first examined the pathological changes in SHRs at different time points (1, 2, and 6 months). We detected a blood pressure elevation and increased infiltration of

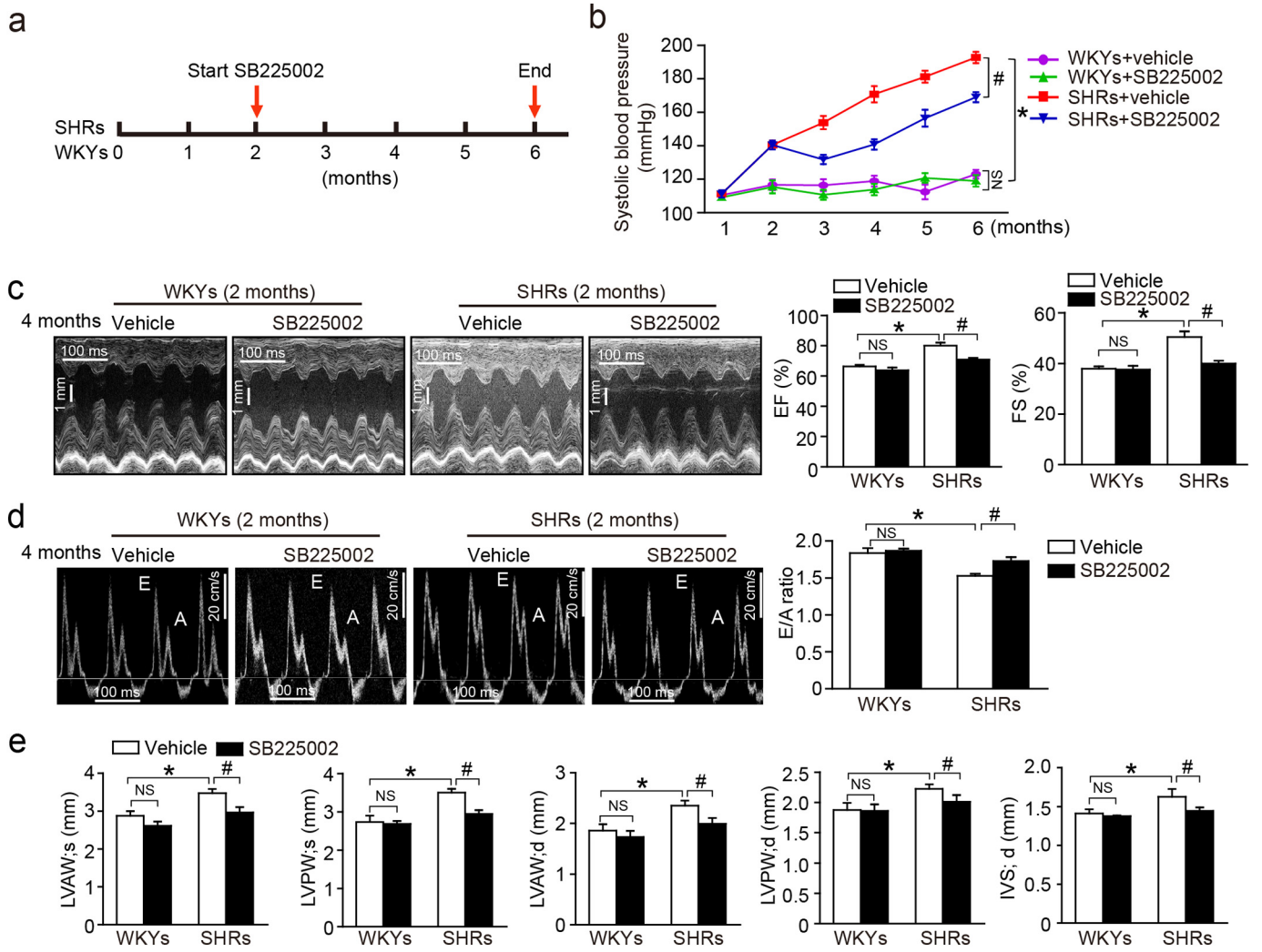

Fig. 2. Administration of CXCR2 inhibitor SB225002 improves hypertension and cardiac dysfunction in SHRs. (a) WKY rats and SHRs at age of 2 months were injected intraperitoneally with CXCR2 inhibitor SB225002 (1 mg/kg/day) or vehicle (DMSO) for additional 4 months. (b) Systolic blood pressure (SBP) was measured every month by tail-cuff method (n = 8). (c) M-mode echocardiography of left ventricular chamber (left), and measurement of ejection fraction (EF) and fractional shortening (FS) (right, n = 8). (d) Pulse-wave Doppler images of mitral inflow from the apical 4-chamber(left), and measurement of E/A ratio (right, n = 8). (e) Measurement of end-systolic and end-diastolic left ventricular anterior wall (LVAW), left ventricular posterior wall (LVPW) and end-diastolic interventricular septum (IVS) (n = 8). Data are presented as means ± SEM, and n represents number of animals, $^{*}P < 0.05$ versus WKY; $^{\#}P < 0.05$ versus SH; $^{ns}P > 0.05$ versus WKY or SHR.

Mac-2^{+} macrophages in the hearts of SHRs at 2 months of age, but we did not detect significant cardiac dysfunction and pathological changes, such as cardiac myocyte hypertrophy and fibrosis in SHR hearts compared with WKYs (Fig. 2, Supplementary Fig. 2a–e and Supplementary Table 3). However, SHRs showed significant hypertension, compensatory cardiac hyperfunction, hypertrophy, fibrosis, and inflammation at 6 months of age (Figs. 2, 3 and 5). Therefore, we administered the CXCR2 inhibitor SB225002 to SHRs and WKY rats at 2 months of age and continued treatment for an additional 4 months. Consistent with our previous findings using from Ang II or DOCA-salt-treated mice [14], SB225002-treated SHRs showed a significant reduction of blood pressure and improved cardiac systolic and diastolic function, reflected by a decreased ejection fraction (EF) and fractional shortening (FS) and increased transmitral E/A ratio compared with those of vehicle-treated SHRs (Fig. 2a–d, Supplementary Tables 2 and 4). Furthermore, dimensions of the end-systolic and end-diastolic left ventricular anterior wall (LVAW), left ventricular posterior wall (LVPW), and interventricular septum (IVS) in SHRs from the SB225002-treated group were also lower than those of the vehicle-treated group (Fig. 2e and Supplementary Table 4). These results suggest that SB225002 treatment is able to attenuate hypertension and myocardial function in SHRs.

3.3. CXCR2 inhibition blunts hypertrophy and fibrosis

Since cardiac hypertrophy develops spontaneously in SHRs arising from increased pressure overload induced by hypertension, we tested whether a CXCR2 inhibitor attenuates cardiac hypertrophy and fibrosis. After 4 months of SB225002 treatment, the increase in heart size and weight indicated by heart weight (HW)/body weight (BW) or tibial length (TL) ratio and myocyte hypertrophy in SHRs were significantly inhibited by SB225002 (Fig. 3a–c). Moreover, severe perivascular and interstitial fibrosis as well as α-SMA-positive myofibroblasts in SHR hearts were substantially suppressed by SB225002 (Fig. 3d–e). The mRNA expression levels of hypertrophic markers (*ANF* and *BNP*) and collagen I/III were also reduced by SB225002 in SHRs (Fig. 3f–g). SB225002 had no impact on WKY rats (Fig. 3a–g). There were no significant differences in myocardial hypertrophy and fibrosis in WKY rats between inhibitor- and vehicle-treated groups (Fig. 3c–g).

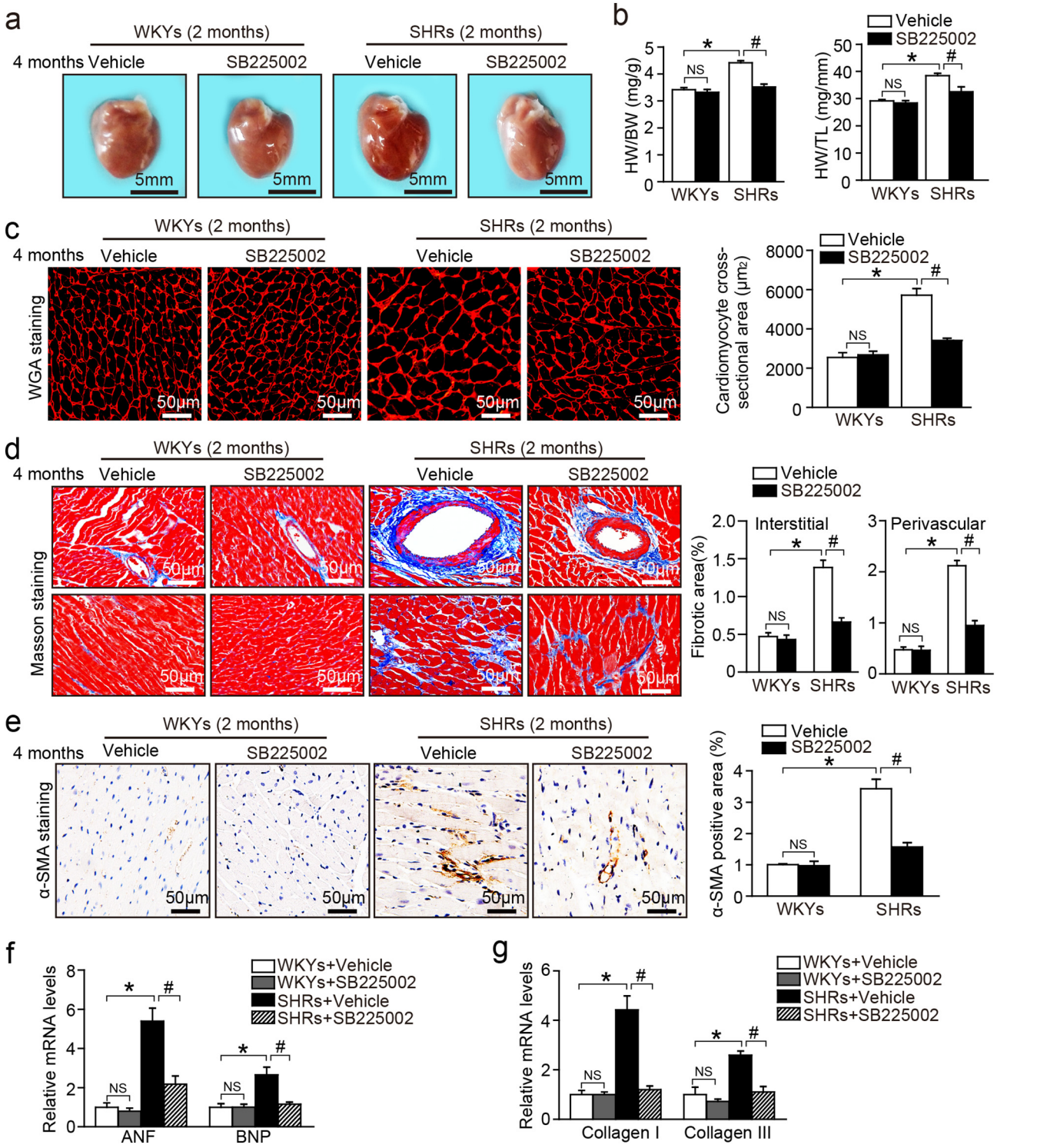

Fig. 3. Inhibition of CXCR2 alleviates cardiac hypertrophy and fibrosis in SHRs. (a) Representative images of heart size. Scale bar: 5 mm. (b) The ratios of heart weight to body weight (HW/BW) and heart weight to tibia length (HW/TL) in each group (right, n = 8). (c) TRITC-labeled WGA staining of heart sections (left), and quantification of cross-sectional area of myocytes (200 cells counted per heart, right, n = 8). (d) Masson's trichrome staining of heart sections (left), and quantification of myocardial interstitial and perivascular collagen deposition (right, n = 6). (e) Immunohistochemical staining of cardiac myofibroblasts with anti-α-SMA antibody (left), and quantification of α-SMA-positive cells (right, n = 6). Scale bar: 50 μm. (f) qPCR analysis of the mRNA levels of ANF and BNP in the heart (n = 6). (g) qPCR analysis of the mRNA levels of collagen I and collagen III in the heart (n = 6). Data are presented as means ± SEM, and n represents number of animals, $^{**}P < 0.05$ versus WKY; $^{\#}P < 0.05$ versus SH; $^{ns}P > 0.05$ versus WKY or SHR.

3.4. Inhibition of CXCR2 inhibits the progression of established cardiac contractile dysfunction, hypertrophy, and fibrosis

To further test whether the inhibition of CXCR2 can attenuate already existing cardiac remodeling, SHRs at the age of 6 months, which had significantly cardiac hypertrophy and fibrosis (Fig. 3), were randomly divided into two groups: one group received SB225002 (1 mg/kg/day) for an additional 5 months and another group received

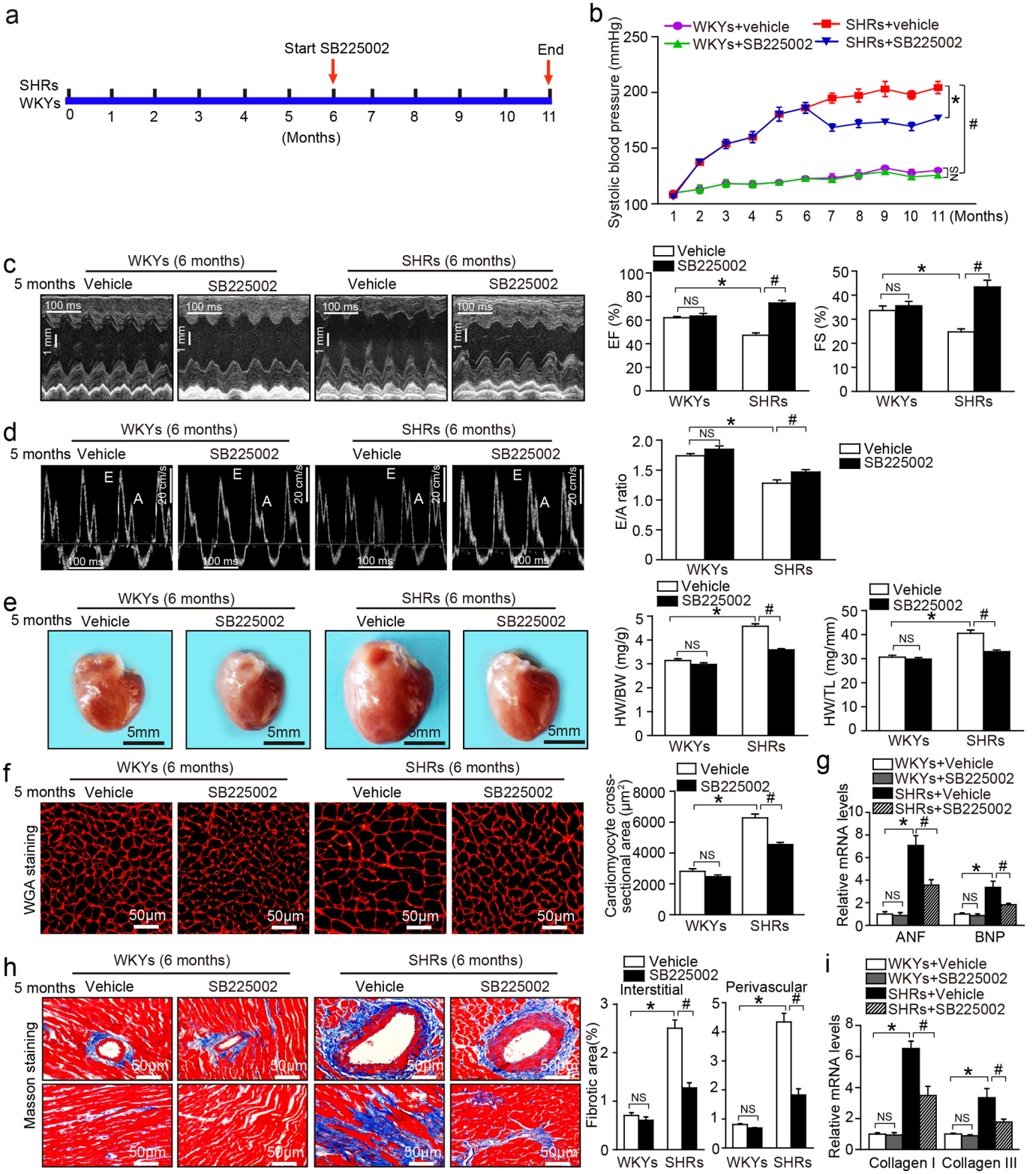

Fig. 4. Chronic inhibition of CXCR2 reverses pre-established cardiac dysfunction, hypertrophy and fibrosis. (a) WKYs and SHRs at age of 6 months were administered with SB225002 (1 mg·kg^{-1} day^{-1}) or vehicle control for additional 5 months. The following experiments were performed the end of 11 months of age. (b) Systolic blood pressure was measured every month by tail-cuff method (n = 8). (c) Representative M-mode echocardiography of left ventricular chamber (left), and assessment of left ventricular EF and FS (right, n = 8). (d) Pulse-wave Doppler images of mitral inflow from the apical 4-chamber(left), and measurement of E/A ratio (right, n = 8). (e) Representative gross images of whole hearts (left). Scale bar: 5 mm. The ratios of heart weight to body weight (HW/BW) and heart weight tibial length (HW/TL) (right, n = 8). (f) Representative images of TRITC-labeled wheat germ agglutinin (WGA) staining to detect cardiac hypertrophy (left). Quantification of the relative myocyte cross-sectional area (n = 6, 200 cells counted per heart; right). (g) qPCR analyses of ANF and BNP mRNA levels (n = 6). (h) Masson's trichrome staining of heart tissues (left), and quantification of myocardial interstitial and perivascular fibrotic area (right, n = 6). Scale bar: 50 μm. (i) qPCR analysis of collagen I and collagen III gene expression levels (n = 6). Data are presented as means ± SEM, and n represents number of animals, $^{*}P < 0.05$ versus WKY; $^{\#}P < 0.05$ versus SH; $^{ns}P > 0.05$ versus WKY or SHR.

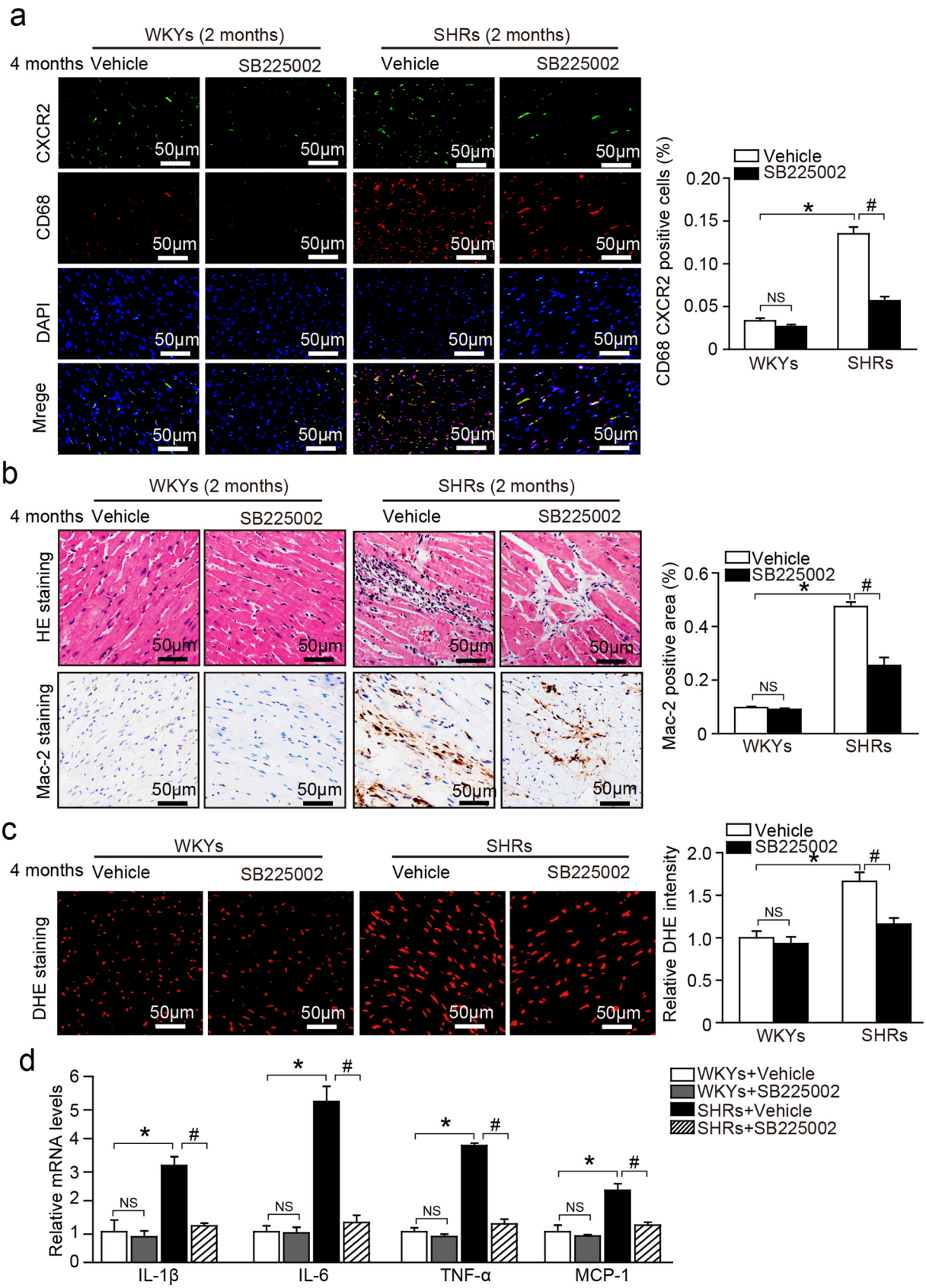

Fig. 5. Blocking CXCR2 activation suppresses myocardial CXCR2$^+$ macrophage infiltration, inflammation and oxidative stress. (a) Double immunofluorescence staining of the heart sections with anti-CXCR2 (green) and anti-CD68 (red) antibodies (left). Nuclei are counterstained with DAPI (blue). The quantification of CXCR2$^+$ and CD68$^+$ positive area (n = 6). (b) Representative images of H&E staining (upper) and immunohistochemical staining of macrophages with anti-Mac-2 antibody (lower), and quantification of Mac-2-positive area (right, n = 6). (c) Dihydroethydium (DHE) staining of heart sections (left), quantification of DHE fluorescence intensity (right, n = 6). (d) qPCR analysis of IL-1β, IL-6, TNF-α, and MCP-1 gene expression levels (n = 6). Scale bar: 50 μm. Data are presented as means ± SEM, and n represents number of animals, $^*P < 0.05$ versus WKY; $^{\#}P < 0.05$ versus SH; $^{ns}P > 0.05$ versus WKY or SHR.

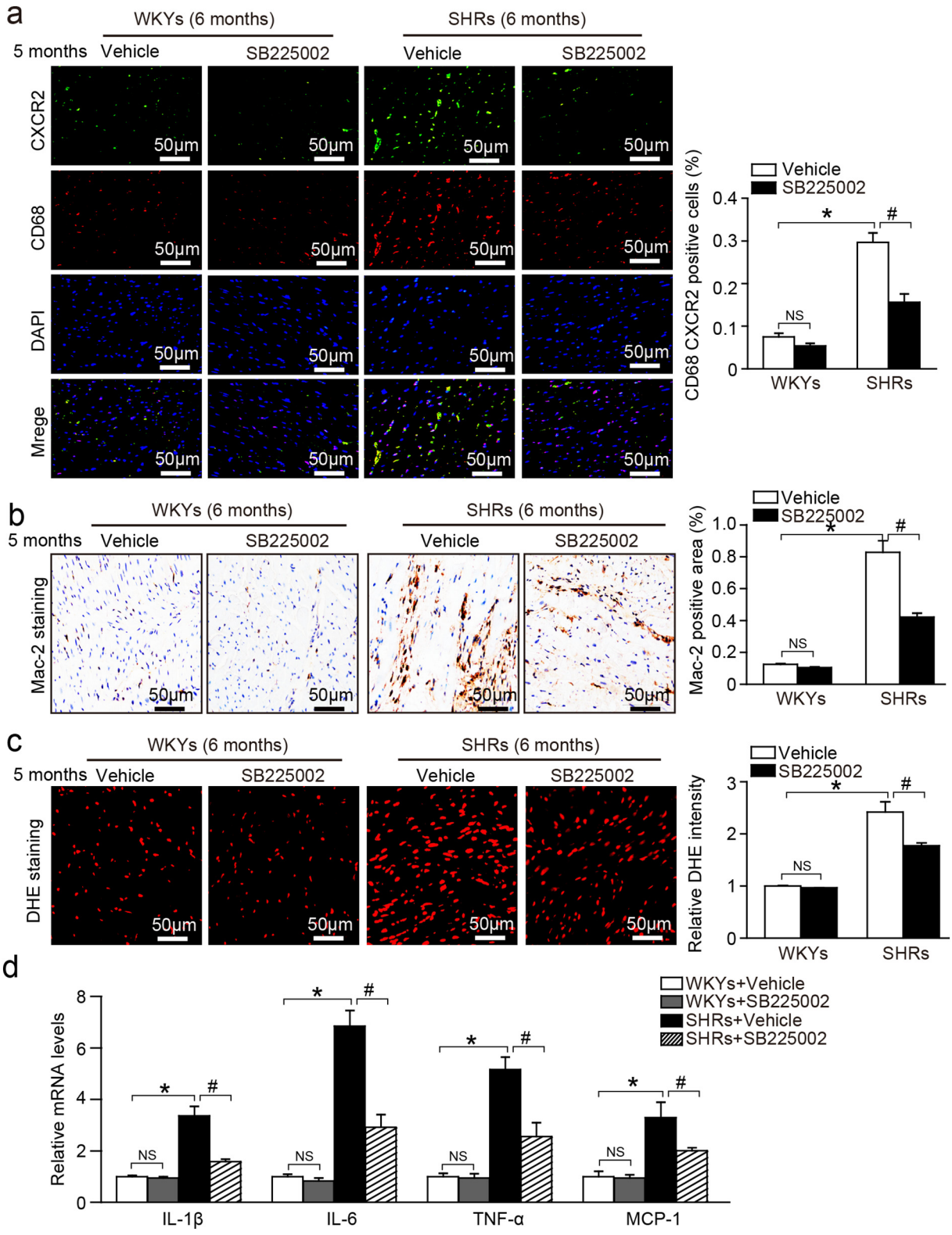

Fig. 6. Chronic blockage of CXCR2 reverses myocardial CXCR2$^+$ macrophage infiltration, inflammatory response and oxidative stress. (a) WKYs and SHRs at age of 6 months were administered with SB225002 (1 mg/kg/day) or vehicle control for additional 5 months. Double immunofluorescence staining of the heart sections with anti-CXCR2 (green) and anti-CD68 (red) antibodies (left). Nuclei are counterstained with DAPI (blue). Quantification of CXCR2+ and CD68+ positive area (n = 6). (b) Immunohistochemical staining of macrophages with anti-Mac-2 antibody (lower), and quantification of Mac-2-positive area (right, n = 6). (c) DHE staining of the heart sections (left), and quantification of DHE fluorescence intensity in fold change (right, n = 6). Scale bar 50 μm. (d) qPCR analysis of IL-1β, IL-6, TNF-α, and MCP-1 mRNA expression (n = 6). Data are presented as means ± SEM, and n represents number of animals, $^*P < 0.05$ versus WKY; $\#P < 0.05$ versus SH; $^{ns}P > 0.05$ versus WKY or SHR.

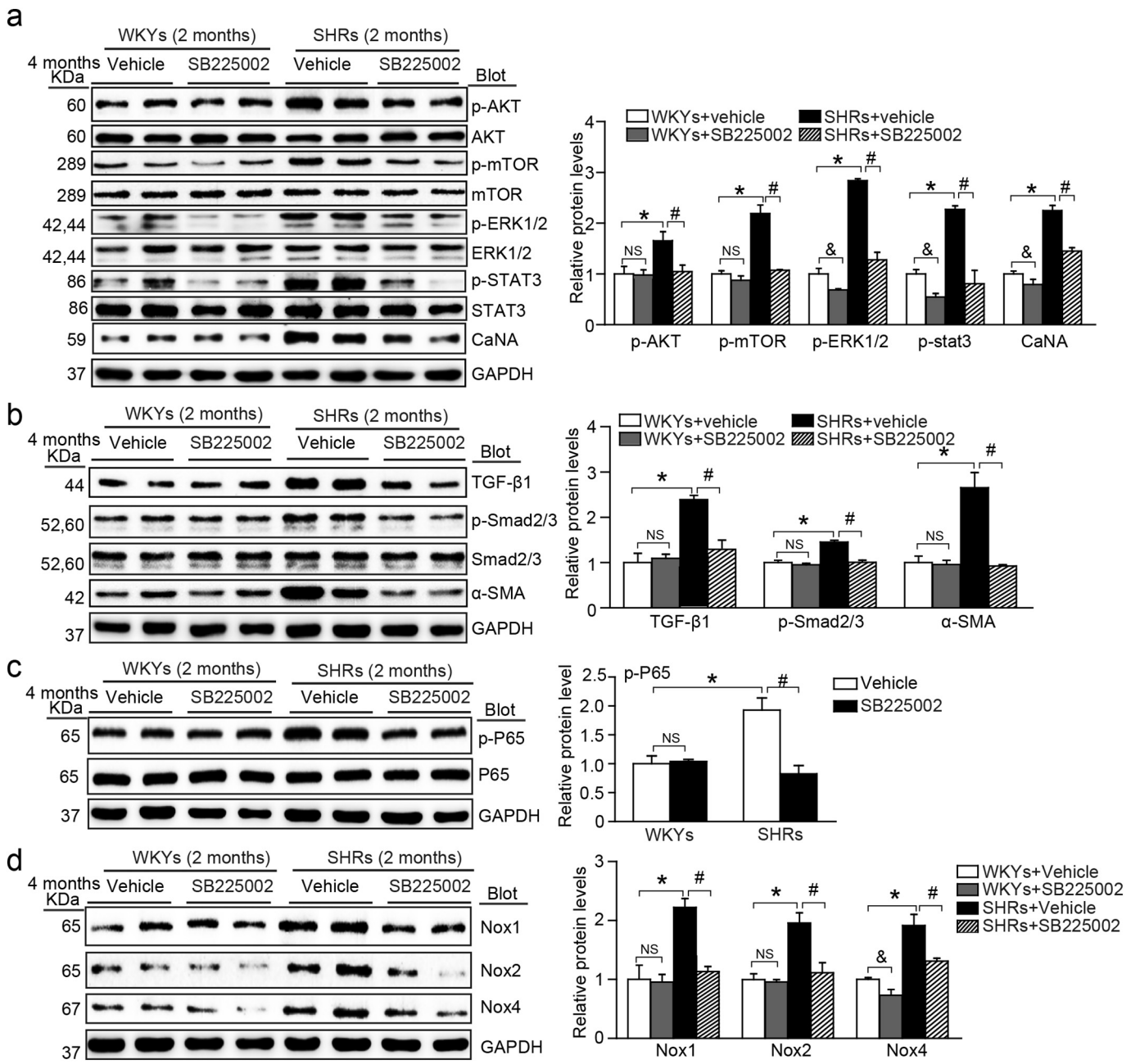

Fig. 7. Administration of SB225002 blunts activation of multiple signaling pathways. (a) Representative immunoblots of p-AKT, AKT, p-mTOR, mTOR, p-ERK, ERK, p-STAT3, STAT3 and calcineurin A (CaNA) in heart tissues from each group (left). Quantification of the relative protein levels by densitometry (right, n = 6). (b) Representative immunoblots of TGF-β1, p-Smad2/3, Smad2/3 and α-SMA (left), and quantification of the relative protein level by densitometry (right, n = 6). (c) Representative immunoblotting analyses of p-P65 and P65 (left), and quantification of the relative protein levels by densitometry (right, n = 6). (d) Representative immunoblots of NOX1, NOX2 and NOX4 (left) and quantification of the relative protein levels by densitometry (right, n = 6). Data are presented as means ± SEM, and n represents number of animals, $^{*}P < 0.05$ versus WKY; $^{\#}P < 0.05$ versus SH; $^{ns}P > 0.05$ versus WKY or SHR.

vehicle only (Fig. 4a). We found that the elevation in blood pressure decreased progressively in SB225002-treated SHRs compared with the vehicle controls (Fig. 4b and Supplementary Table 2). Moreover, the treatment of SHRs with SB225002 significantly reversed cardiac systolic and diastolic dysfunction (decreased EF, FS, and E/A ratio), cardiac hypertrophy (increase of heart size, HW/BW, and HW/TL ratios), cross-sectional area of myocytes, mRNA expression of ANF, BNP, and collagen (I/III) and myocardial fibrosis compared with those in vehicle-treated SHRs within 5 months of treatment (Fig. 4c–i and Supplementary Table 5). There were no significant differences in these parameters in WKY rats between inhibitor- and vehicle-treated groups (Fig. 4b–i and Supplementary Table 5). These results indicate that the blockade of CXCR2 ameliorates established hypertension, cardiac remodeling and dysfunction.

3.5. Blockage of CXCR2 attenuates myocardial CXCR2^{+} cell infiltration, inflammatory responses and oxidative stress

To determine whether CXCR2 inhibition the affects inflammatory response and oxidative stress, we examined the infiltration of CXCR2^{+} proinflammatory cells in the heart. Consistent with the results obtained for CXCR2$^{-/-}$ or inhibitor-treated mice [13], the administration of SB225002 to SHRs significantly attenuated the number of CD68^{+}CXCR2^{+} macrophages in the hearts compared with vehicle-

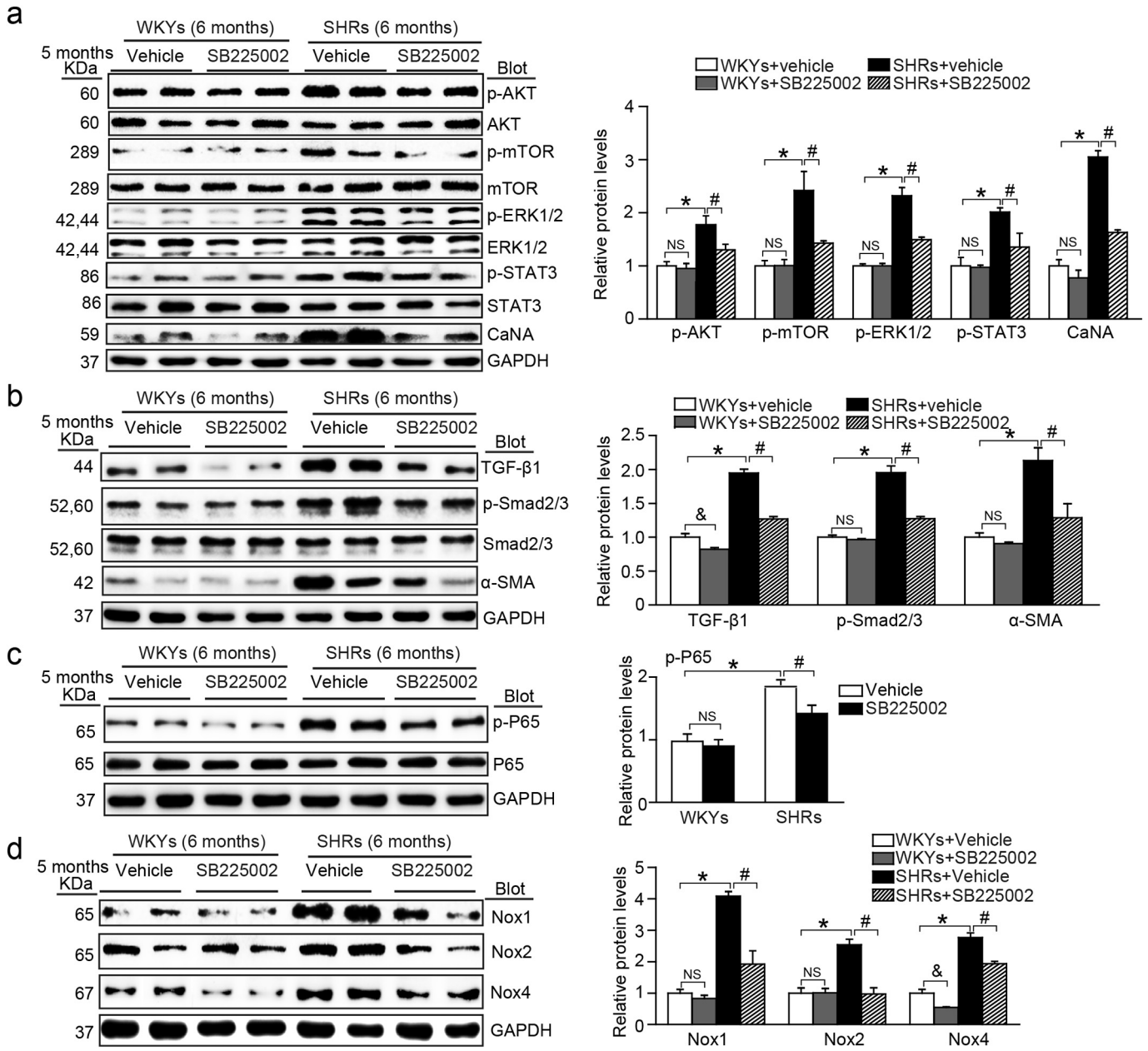

Fig. 8. SB225002 treatment reverses the activation of multiple signaling pathways in SHRs. (a) WKYs and SHRs at age of 6 months were administered with SB225002 (1 mg/kg/day) or vehicle control for additional 5 months. Representative immunoblots of p-AKT, AKT, p-mTOR, mTOR, p-ERK, ERK, p-STAT3, STAT3 and calcineurin A (CaNA) in heart tissues from each group (left). Quantification of the relative protein levels by densitometry (right, n = 6). (b) Representative immunoblots of TGF-β1, p-Smad2/3, Smad2/3 and α-SMA (left), and quantification of the relative protein levels (right, n = 6). (c) Representative immunoblots of p-P65 and P65 (left), and quantification of the relative protein levels (right, n = 6). (d) Representative immunoblots of NOX1, NOX2 and NOX4 (left), and quantification of the relative protein levels (right, n = 6). Data are presented as means ± SEM, and n represents number of animals, $^{*}P < 0.05$ versus WKY; $^{\#}P < 0.05$ versus SH; $^{ns}P > 0.05$ versus WKY or SHR.

treated controls (Fig. 5a). Myocardial recruitment of pro-inflammatory cells, including Mac-2^{+} macrophages, and the expression of IL-1β, IL-6, TNF-α and monocyte chemoattractant protein-1(MCP-1) compared with were markedly lower for SHRs treated with SB225002 than with vehicle (Fig. 5b, d). Increased vascular permeability leads to macrophage infiltration in the heart [22]. We tested the effect of SB225002 on zona occludens-1 (ZO-1) expression, an endothelial tight junction protein required for vascular permeability [23]. Immunostaining showed that ZO-1 fluorescence intensity in the heart vessels was significantly decreased in vehicle-treated SHRs, and this effect was reversed in SB225002-treated mice (Supplemental Fig. 3a). Immunoblotting confirmed that the reduction of ZO-1 protein levels in vehicle-treated SHRs was also attenuated in SB225002-treated mice (Supplemental Fig. 3b), suggesting that SB225002 treatment also improves vascular permeability in SHR hearts. In addition, the level of myocardial superoxide production, as indicated by DHE staining, was lower in SB225002-treated SHRs than in vehicle-treated controls (Fig. 5c).

We next evaluated whether CXCR2 inhibition attenuates pre-established inflammation and oxidative stress. The increased accumulation of CD68^{+}CXCR2^{+} cells, Mac-2-positive macrophages, and superoxide production were markedly reversed in SB225002-treated SHRs compared with vehicle-treated SHRs (Fig. 6a–d). Taken together, these results demonstrate that blocking CXCR2 can prevent and reverse CXCR2-mediated inflammation and oxidative stress.

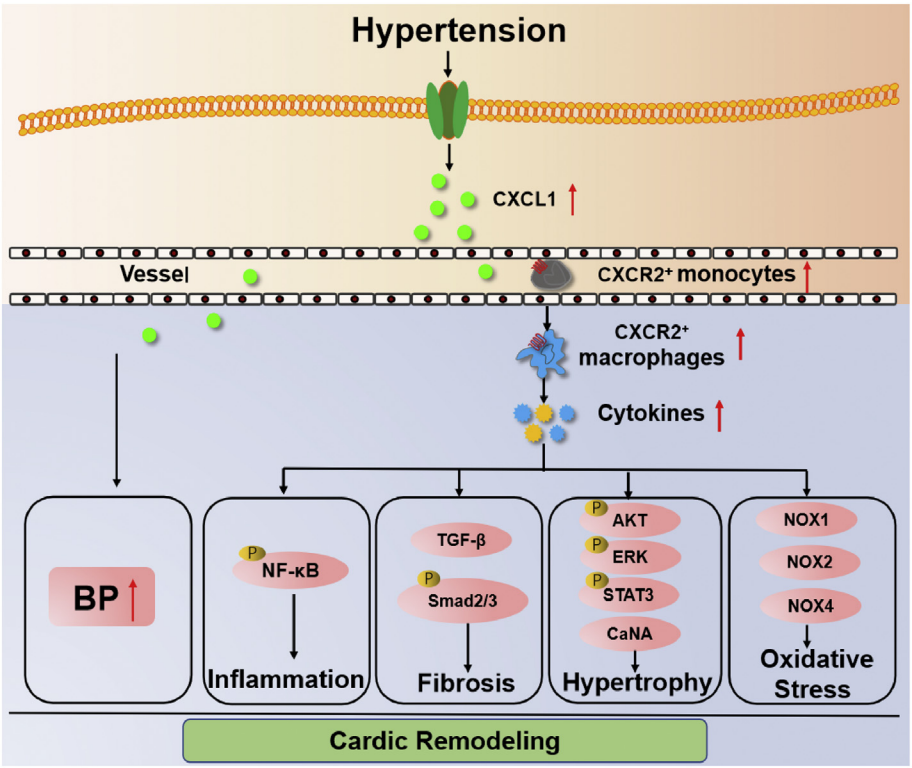

Fig. 9. A working model for CXCL1 to recruit CXCR2$^+$ macrophages into the vessel and heart, which initiates hypertension, inflammation, oxidative stress to induce cardiac hypertrophy and fibrosis thereby leading to cardiac remodeling in hypertensive rats. Conversely, inhibition of CXCR2 by inhibitor SB225002 attenuates these effects.

3.6. Administration of SB225002 blunts activation of multiple signaling pathways

To elucidate the molecular mechanism by which CXCR2 inhibition improves cardiac remodeling and dysfunction, we examined multiple signaling pathways with known roles in cardiac remodeling, inflammation, and oxidative stress [13]. Treatment of SHRs with SB225002 significantly reduced the protein levels of hypertrophic signaling molecules (p-AKT, p-mTOR, p-ERK1/2, p-STAT3, and calcineurin A), fibrotic signaling molecules (TGF-β and p-Smad2/3), a key regulator of cytokine expression (NF-κB-p-p65), and nicotinamide adenine dinucleotide phosphate (NADPH) oxidase isoforms (NOX1, NOX2, and NOX4) in hearts compared with the vehicle treatment (Fig. 7a–d). Similarly, the activation of these signaling pathways was reversed by SB225002 treatment in SHRs (Fig. 8a–d). Together, these results indicate that CXCR2 inhibition attenuates hypertensive cardiac remodeling-related signaling pathways.

3.7. Discussion and conclusions

We provide novel evidence demonstrating that the inhibition of CXCR2 attenuates progression of cardiac hypertrophic remodeling cardiac remodeling and dysfunction in SHRs. These results verify our previous findings from CXCR2 knockout mice and wild-type mice treated with the CXCR2 specific inhibitor SB265610 [13]. The present data confirm that blocking CXCR2 reduces the myocardial recruitment of monocytes/macrophages and the production of proinflammatory cytokines and ROS, which suppresses the activation of multiple signaling pathways, leading to the inhibition of cardiac remodeling and dysfunction. These findings are summarized in Fig. 9. Overall, these data provide new insights into the potential clinical application of CXCR2 inhibitors for the treatment of hypertensive heart diseases.

The recruitment of monocytes/macrophages is a key event in the development of different immune diseases [24,25]. Various adhesion molecules and chemokines are involved in the mobilization and recruitment of proinflammatory cells [26]. CXCR2, the chemokine receptor for CXCL1, CXCL2, CXCL3, CXCL5, CXCL7, and CXCL8 in mice, is critically involved in this process and the regulation of immune-mediated inflammatory diseases in different models [27–30]. Increasing evidence suggests that CXCR2 and its ligands are responsible for recruiting monocytes/macrophages and neutrophils into injured tissues; they have also been implicated in various cardiovascular diseases, including myocardial infarction, atherosclerosis, and acute aortic dissection [9,12,31]. CXCR2 is important in inflammatory responses and oxidative stress, by stimulating a variety of cell signaling pathways, including NF-κB, AKT/mTOR, ERK1/2, STAT3, calcineurin A, and TGF-β/Smad2/3, leading to cardiac remodeling and dysfunction. The genetic ablation of CXCR2 significantly blocks the recruitment of monocytes/macrophages into vascular and heart tissues and improves these effects in Ang II-induced mouse models [13,14]. Consistent with these findings, the present study further confirmed that the chronic inhibition of CXCR2 activity by SB225002 had similar effects in SHRs (Figs. 2–8). Thus, selectively interfering with CXCR2 represents a novel therapeutic approach to prevent and treat hypertension and cardiac remodeling.

Several CXCR2-specific inhibitors such as reparixin (also known as Repertaxin), CX797, and SB265610, have attracted increased attention owing to their anticancer, anti-inflammatory, and antioxidative activity. Accumulating data suggest that CXCR2 inhibitors exert beneficial effects by different mechanisms. Reparixin protects against ischemia-reperfusion lung injury via the reduction of intracellular free calcium and reactive oxygen species [32]. CX797 inhibits IL-8-mediated cell migration, cyclic adenosine monophosphate (cAMP) signaling and receptor degradation by the upregulation of β-arrestin-2 recruitment [33]. SB265610, an allosteric inverse agonist blocks CXCR2 activation by interfering with G protein coupling [34]. Indeed, these inhibitors have been examined in various animal disease models and play protective roles in autoimmune diseases, ischemia-reperfusion injury, diabetes, lung injury, and vascular injury [30,31,35–37]. Our recent results also demonstrate that the administration of CXCR2 inhibitor SB265610 markedly reduces Ang II-induced hypertension and vascular dysfunction, and suppresses Ang II-induced cardiac inflammation and remodeling in mice through blood-dependent and independent

manners [13,14]. Consistent with these observations [14], SB225002 treatment attenuated hypertension development and prevented cardiac inflammation and remodeling accompanied by the inhibition of NF-κB, AKT, ERK1/2, calcineurin and TGF-β/Smad2/3 signaling pathways in SHRs (Figs. 7–8). Although no CXCR2 inhibitors are clinically approved, a pilot study further demonstrates that the administration of reparixin significantly reduces the number of neutrophil granulocytes in the blood in patients undergoing on-pump coronary artery bypass grafting (CABG) and appears to be feasible and safe [35]. Thus, our results for SHRs suggest the potential clinical use of CXCR2 inhibitors for the treatment of hypertension and cardiac remodeling.

In conclusion, our observations demonstrate for the first time that the chronic blockage of CXCR2 with SB225002 significantly attenuates and reverses monocyte infiltration into injured hearts, resulting in marked reductions of proinflammatory cytokines and oxidative stress and an improvement in cardiac remodeling in SHRs, supporting their use as a chronic therapy. Moreover, our data demonstrate the central role of CXCR2 in mediating monocyte recruitment and their sequelae during hypertension in SHRs. Thus, our findings have clinical implications given the high prevalence of hypertension and HF and should facilitate future studies of the effects of CXCR2 inhibition on hypertensive heart disease in humans.

Supplementary data to this article can be found online at https://doi.org/10.1016/j.bbadis.2019.165551.

Transparency document

The https://doi.org/10.1016/j.bbadis.2019.165551 associated with this article can be found, in online version.

Author contributions

Y.L.Z., C.G., J.Y., P.B.L., L.X.Z., and C.C. conceived of the experiments, the acquisition of the data and analysis and interpreted the data. Y.L.Z. and C.G. participated in the statistical analysis of the primary data. S.B.G., H.H.L. and Y.L. drafted the manuscript. H.H.L. and Y.L. provided funding to support the study. H.H.L. supervised the study. All authors approved the final version of the manuscript.

Declaration of competing interest

The authors declare no conflicts of interest.

Acknowledgments

This work was supported by grants from the State Key Program of National Natural Science Foundation of China 81630009 (H.H.L.), the Youth Science Fund Program of National Natural Science Foundation of China 81400247 (Y.L.), Dalian High-Level Talents Innovation and Entrepreneurship Projects 2015R019 (H.H.L.), and the Chang Jiang Scholar Program of China T2011160 (H.H.L.).

References

[1] E.Z. Soliman, R.J. Prineas, Antihypertensive therapies and left ventricular hypertrophy, Curr. Hypertens. Rep. 19 (2017) 79.
[2] M. Nakamura, J. Sadoshima, Mechanisms of physiological and pathological cardiac hypertrophy, Nat. Rev. Cardiol. 15 (2018) 387–407.
[3] A.M. Rababa'h, A.N. Guillory, R. Mustafa, T. Hijjawi, Oxidative stress and cardiac remodeling: an updated edge, Curr. Cardiol. Rev. 14 (2018) 53–59.
[4] N. Li, H.X. Wang, Q.Y. Han, W.J. Li, Y.L. Zhang, J. Du, Y.L. Xia, H.H. Li, Activation of the cardiac proteasome promotes angiotension II-induced hypertrophy by down-regulation of ATRAP, J. Mol. Cell. Cardiol. 79 (2015) 303–314.
[5] L. Wang, Y.L. Li, C.C. Zhang, W. Cui, X. Wang, Y. Xia, J. Du, H.H. Li, Inhibition of Toll-like receptor 2 reduces cardiac fibrosis by attenuating macrophage-mediated inflammation, Cardiovasc. Res. 101 (2014) 383–392.
[6] S. Liu, L.X. Liu, Y.L. Zhang, S. Lai, Y.P. Xie, N.N. Li, H.X. Wang, Y.L. Xia, Y. Liu, H.H. Li, Cardiac ablation of SOCS3 aggravates DOCA-salt-induced hypertrophic remodeling by activation of Gp130-dependent signaling in mice, Cellular Physiology and Biochemistry: International Journal of Experimental Cellular Physiology, Biochemistry, and Pharmacology 47 (2018) 140–150.
[7] N. He, Q.H. Gong, F. Zhang, J.Y. Zhang, S.X. Lin, H.H. Hou, Q. Wu, A.S. Sun, Evodiamine inhibits angiotensin II-induced rat cardiomyocyte hypertrophy, Chinese Journal of Integrative Medicine 24 (2018) 359–365.
[8] D.T. Graves, Y. Jiang, Chemokines, a family of chemotactic cytokines, Critical Reviews in Oral Biology and Medicine: An Official Publication of the American Association of Oral Biologists 6 (1995) 109–118.
[9] S.T. Tarzami, W. Miao, K. Mani, L. Lopez, S.M. Factor, J.W. Berman, R.N. Kitsis, Opposing effects mediated by the chemokine receptor CXCR2 on myocardial ischemia-reperfusion injury: recruitment of potentially damaging neutrophils and direct myocardial protection, Circulation 108 (2003) 2387–2392.
[10] A.M. Ritzman, J.M. Hughes-Hanks, V.A. Blaho, L.E. Wax, W.J. Mitchell, C.R. Brown, The chemokine receptor CXCR2 ligand KC (CXCL1) mediates neutrophil recruitment and is critical for development of experimental Lyme arthritis and carditis, Infect. Immun. 78 (2010) 4593–4600.
[11] W.A. Boisvert, R. Santiago, L.K. Curtiss, R.A. Terkeltaub, A leukocyte homologue of the IL-8 receptor CXCR-2 mediates the accumulation of macrophages in atherosclerotic lesions of LDL receptor-deficient mice, J. Clin. Invest. 101 (1998) 353–363.
[12] O. Soehnlein, M. Drechsler, Y. Doring, D. Lievens, H. Hartwig, K. Kemmerich, A. Ortega-Gomez, M. Mandl, S. Vijayan, D. Projahn, C.D. Garlichs, R.R. Koenen, M. Hristov, E. Lutgens, A. Zernecke, C. Weber, Distinct functions of chemokine receptor axes in the atherogenic mobilization and recruitment of classical monocytes, EMBO Molecular Medicine 5 (2013) 471–481.
[13] L. Wang, Y.L. Zhang, Q.Y. Lin, Y. Liu, X.M. Guan, X.L. Ma, H.J. Cao, Y. Liu, J. Bai, Y.L. Xia, J. Du, H.H. Li, CXCL1-CXCR2 axis mediates angiotensin II-induced cardiac hypertrophy and remodelling through regulation of monocyte infiltration, Eur. Heart J. 39 (2018) 1818–1831.
[14] L. Wang, X.C. Zhao, W. Cui, Y.Q. Ma, H.L. Ren, X. Zhou, J. Fassett, Y.Z. Yang, Y. Chen, Y.L. Xia, J. Du, H.H. Li, Genetic and pharmacologic inhibition of the chemokine receptor CXCR2 prevents experimental hypertension and vascular dysfunction, Circulation 134 (2016) 1353–1368.
[15] T. Ishimitsu, T. Honda, E. Ohno, S. Furukata, Y. Sudo, N. Nakano, T. Takahashi, H. Ono, H. Matsuoka, Year-long antihypertensive therapy with candesartan completely prevents development of cardiovascular organ injuries in spontaneously hypertensive rats, Int. Heart J. 51 (2010) 359–364.
[16] L. Zhang, X. Yan, Y.L. Zhang, J. Bai, T.H. Hidru, Q.S. Wang, H.H. Li, Vitamin D attenuates pressure overload-induced cardiac remodeling and dysfunction in mice, J. Steroid Biochem. Mol. Biol. 178 (2018) 293–302.
[17] T. Shimizu, N. Narang, P. Chen, B. Yu, M. Knapp, J. Janardanan, J. Blair, J.K. Liao, Fibroblast deletion of ROCK2 attenuates cardiac hypertrophy, fibrosis, and diastolic dysfunction, JCI Insight 2 (2017).
[18] Y. Nishijima, A. Sridhar, I. Bonilla, M. Velayutham, M. Khan, R. Terentyeva, C. Li, P. Kuppusamy, T.S. Elton, D. Terentyev, S. Gyorke, J.L. Zweier, A.J. Cardounel, C.A. Carnes, Tetrahydrobiopterin depletion and NOS2 uncoupling contribute to heart failure-induced alterations in atrial electrophysiology, Cardiovasc. Res. 91 (2011) 71–79.
[19] Y.L. Zhang, L.Y. Zhi, L.X. Zou, C. Chen, J. Bai, Q.Y. Lin, S. Lai, L. Wang, Y. Liu, H.H. Li, Analysis of genes related to angiotensin II-induced arterial injury using a time series microarray, Cellular Physiology and Biochemistry: International Journal of Experimental Cellular Physiology, Biochemistry, and Pharmacology 48 (2018) 983–992.
[20] C. Chen, L.X. Zou, Q.Y. Lin, X. Yan, H.L. Bi, X. Xie, S. Wang, Q.S. Wang, Y.L. Zhang, H.H. Li, Resveratrol as a new inhibitor of immunoproteasome prevents PTEN degradation and attenuates cardiac hypertrophy after pressure overload, Redox Biol. 20 (2018) 390–401.
[21] V.W. Dolinsky, A.Y. Chan, I. Robillard Frayne, P.E. Light, C. Des Rosiers, J.R. Dyck, Resveratrol prevents the prohypertrophic effects of oxidative stress on LKB1, Circulation 119 (2009) 1643–1652.
[22] C. Yang, A. Tian, J. Wu, Z. Meng, Y. Zhang, G. Nie, Z. Li, Gold nanoparticles for targeting the fibrotic heart: a probe indicating vascular permeability, J. Nanosci. Nanotechnol. 19 (2019) 7546–7550.
[23] A. Muthusamy, C.M. Lin, S. Shanmugam, H.M. Lindner, S.F. Abcouwer, D.A. Antonetti, Ischemia-reperfusion injury induces occludin phosphorylation/ubiquitination and retinal vascular permeability in a VEGFR-2-dependent manner, Journal of Cerebral Blood Flow and Metabolism: Official Journal of the International Society of Cerebral Blood Flow and Metabolism 34 (2014) 522–531.
[24] K.C. Navegantes, R. de Souza Gomes, P.A.T. Pereira, P.G. Czaikoski, C.H.M. Azevedo, M.C. Monteiro, Immune modulation of some autoimmune diseases: the critical role of macrophages and neutrophils in the innate and adaptive immunity, J. Transl. Med. 15 (2017) 36.
[25] C. Shi, E.G. Pamer, Monocyte recruitment during infection and inflammation, Nat. Rev. Immunol. 11 (2011) 762–774.
[26] T. Garrood, L. Lee, C. Pitzalis, Molecular mechanisms of cell recruitment to inflammatory sites: general and tissue-specific pathways, Rheumatology 45 (2006) 250–260.
[27] T.S. Olson, K. Ley, Chemokines and chemokine receptors in leukocyte trafficking, American Journal of Physiology. Regulatory, Integrative and Comparative Physiology 283 (2002) R7–28.
[28] M.M. Barsante, T.M. Cunha, M. Allegretti, F. Cattani, F. Policani, C. Bizzarri, W.L. Tafuri, S. Poole, F.Q. Cunha, R. Bertini, M.M. Teixeira, Blockade of the chemokine receptor CXCR2 ameliorates adjuvant-induced arthritis in rats, Br. J. Pharmacol. 153 (2008) 992–1002.
[29] M. Veenstra, R.M. Ransohoff, Chemokine receptor CXCR2: physiology regulator and neuroinflammation controller? J. Neuroimmunol. 246 (2012) 1–9.
[30] F.M. Konrad, J. Reutershan, CXCR2 in acute lung injury, Mediat. Inflamm. 2012

(2012) 740987.
[31] A. Anzai, M. Shimoda, J. Endo, T. Kohno, Y. Katsumata, T. Matsuhashi, T. Yamamoto, K. Ito, X. Yan, K. Shirakawa, R. Shimizu-Hirota, Y. Yamada, S. Ueha, K. Shinmura, Y. Okada, K. Fukuda, M. Sano, Adventitial CXCL1/G-CSF expression in response to acute aortic dissection triggers local neutrophil recruitment and activation leading to aortic rupture, Circ. Res. 116 (2015) 612–623.
[32] R. Bertini, M. Allegretti, C. Bizzarri, A. Moriconi, M. Locati, G. Zampella, M.N. Cervellera, V. Di Cioccio, M.C. Cesta, E. Galliera, F.O. Martinez, R. Di Bitondo, G. Troiani, V. Sabbatini, G. D'Anniballe, R. Anacardio, J.C. Cutrin, B. Cavalieri, F. Mainiero, R. Strippoli, P. Villa, M. Di Girolamo, F. Martin, M. Gentile, A. Santoni, D. Corda, G. Poli, A. Mantovani, P. Ghezzi, F. Colotta, Noncompetitive allosteric inhibitors of the inflammatory chemokine receptors CXCR1 and CXCR2: prevention of reperfusion injury, Proc. Natl. Acad. Sci. U. S. A. 101 (2004) 11791–11796.
[33] H. Ha, N. Neamati, Pyrimidine-based compounds modulate CXCR2-mediated signaling and receptor turnover, Mol. Pharm. 11 (2014) 2431–2441.
[34] M.E. Bradley, M.E. Bond, J. Manini, Z. Brown, S.J. Charlton, SB265610 is an allosteric, inverse agonist at the human CXCR2 receptor, Br. J. Pharmacol. 158 (2009) 328–338.
[35] P. Opfermann, U. Derhaschnig, A. Felli, J. Wenisch, D. Santer, A. Zuckermann, M. Dworschak, B. Jilma, B. Steinlechner, A pilot study on reparixin, a CXCR1/2 antagonist, to assess safety and efficacy in attenuating ischaemia-reperfusion injury and inflammation after on-pump coronary artery bypass graft surgery, Clin. Exp. Immunol. 180 (2015) 131–142.
[36] A. Citro, A. Valle, E. Cantarelli, A. Mercalli, S. Pellegrini, D. Liberati, L. Daffonchio, O. Kastsiuchenka, P.A. Ruffini, M. Battaglia, M. Allegretti, L. Piemonti, CXCR1/2 inhibition blocks and reverses type 1 diabetes in mice, Diabetes 64 (2015) 1329–1340.
[37] A. Zarbock, M. Allegretti, K. Ley, Therapeutic inhibition of CXCR2 by Reparixin attenuates acute lung injury in mice, Br. J. Pharmacol. 155 (2008) 357–364.